# Device for Force Measurement in Non-Invasive Mouse ACL Injury Models: A Low-Cost and Portable Alternative

Nejat Can
Department of Biomedical Engineering
University of Rochester
Rochester, NY, USA
ncan@u.rochester.edu

***Abstract*—Osteoarthritis and anterior cruciate ligament (ACL) injury have shown to be linked but poorly understood. Animal models are essential for understanding ACL injury, and there are a variety of models that have been developed. This study aims to introduce a new injury device that is significantly lower in cost and highly portable, suggesting ease of accessibility and better application for *in situ* studies. Computer-aided-design and 3D printing was used to precisely manufacture parts that encase an aluminum beam. The beam was fitted with a strain gauge, which was connected to a circuit that outputs a digital value proportional to strain. The relationship between the load on the beam and digital output was characterized by an experiment. The results indicated that digital output can confidently predict the load applied due to a linear relationship ($R^2$=*0.9983* and $p<0.001$). An *in vivo* non-invasive ACL injury experiment was done in accordance with our model, and results indicated that mean force at ACL rupture (14.62 N, SD = 3.00 N) and difference between males and females were consistent with previously published results. Results indicate that our model can be used to investigate ACL injury and post-traumatic osteoarthritis in mouse specimens.**

***Keywords*—ACL injury, injury model, device, non-invasive, osteoarthritis**

## I. Introduction

ACL injury is common and often leads to post-traumatic osteoarthritis (PTOA). The incidence rate of ACL injury resulting in surgery and not resulting in surgery is 36.9 and 1147 per 100,000 person-years respectively [1]. Upon ACL injury, the reported incidence of PTOA is as high as 87% [2]. Mouse models are one of the most prevalent animal models used for understanding ACL injury [3]. To achieve a reliable and consistent injury model, ACL rupture can be used as an indicator of ACL injury in mice specimens.

ACL rupture can be caused by a variety of methods. One possible method is surgical ACL transection, which involves an incision through the skin and joint capsule, allowing for the ACL to be cut with another incision [4]. However, invasive models like these require surgical expertise and differ significantly than the most common cause of ACL rupture occurring in humans, which is due to acute mechanical loads on the knee. In order to counter these limitations, non-invasive models have been developed. Non-invasive models do not require surgical expertise and cause ACL rupture via mechanical loads. The scope of this paper will involve the model developed by Christiansen et al. [5] which is a reliable model resulting in no macroscopic damage to surrounding ligaments of the knee, such as PCL or MCL [4].

The model developed by Christiansen et al. counters the limitations of invasive models, however it comes with its own limitations. Load-based non-invasive models require high-precision electromagnetic materials testing machines [5,6]. Materials testing machines are expensive and immobile. The high cost makes laboratory access harder and the immobility renders *in situ* experiments hard to execute. To counter these limitations, a low cost and portable device has been designed in the current study, and open access .stl files and circuit diagrams have been provided on GitHub [7]. The device measures axial force by utilizing a half-bridge strain gauge integrated into a handheld tool. Device effectiveness was tested with an *in vivo* mouse experiment and results indicate successful emulation of the Christiansen et al. model.

## II. Materials and Methods

### A. Design Requirements

In order to emulate the materials testing machine, the device must measure and store force data during ACL injury. The device must also be small and portable, as well as low-cost, in order to counter the limitations of the typical non-invasive ACL injury model. The device should require no surgical expertise to operate, as well as being easy to disinfect.

The mean compressive force at ACL rupture for mice was 10.19 N. Therefore, the device should be rated for a maximum load that will account for the load requirements. Assuming outliers exceed this average by roughly two-fold, the device must measure up to 20 N. A factor of safety for reliable force measurement was determined as F.S=2.5, rating the device at 50 N. The factor of safety for device failure was rated at 5.0, for a minimum failure load at 100 N.

The force must be measured reliably, meaning that ambient conditions such as temperature should not affect the force reading. The force must be applied via a flat smooth surface that emulates that of other non-invasive ACL injury models.

### B. Design

TABLE I: Tools and Materials

| Tool/Material | Detail/Description |
|---|---|
| 3D printer | Minimum print vol.: 50x50x120 mm |
| Microcontroller | Arduino Uno |
| HX711 Load Cell Amplifier | N/A |
| Aluminum beam | Strain will occur on this beam |
| Strain gauge | Small area ($\leq$0.4 mm$^2$) |

The device was designed with an aluminum beam with a half-bridge strain gauge integrated on it. The beam was secured to two 3D printed parts (Fig. 1) that were designed carefully to satisfy the Design Requirements. Computer-aided-design and 3D printing were utilized for a high precision manufacturing process. This structure was coupled with a circuit which was designed to yield a digital output that is linearly proportional to the load at the the aluminum beam (Fig. 2).

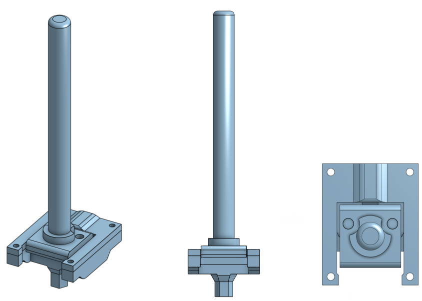

Fig. 1: CAD view of structure encasing the aluminum beam.

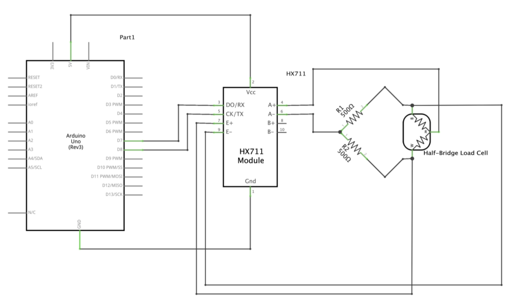


Fig. 2: Fritzing sketch of device circuitry with Arduino and half-bridge strain gauge

After the device was assembled, it was calibrated in order to quantify the linear relationship between digital output and load at the beam. To achieve calibration, known loads were applied to the device and the digital output was recorded over a 15 second period. This process was repeated for 12 different loads ranging from 0 to 22 N. The sampling rate of the device is 10.7 Hz, the digital output data points for each periodical load application was averaged, resulting in one digital output value per known load. A linear equation was acquired by applying simple linear regression in MATLAB via the `polyfit(x,y,n)` function.

$$Force(x) = (0.015734 * x - 1.6638) \quad (1)$$

Equation 1 indicated a very strong linear relationship ($R^2 = 0.9983$ and $p<0.001$). The equation yields the load at the beam for input x, that is, the digital output of the device. Fig. 3 shows the linear regression.

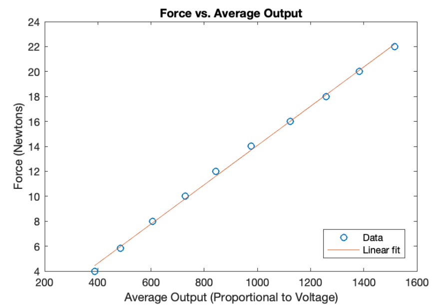


Fig. 3: Calibration Graph

### C. In Vivo Non-Invasive ACL Injury Experiment

*1) Ethics:* All experiments were conducted while following animal experiment ethics rules and regulations at University of Rochester Medical Center. The current study is interested in the process of causing *in vivo* ACL injury, however after injury the specimens were still used for a longitudinal experiment as part of another study.

*2) Method:* The injury model of Christiansen et al. involves an axial compression of the lower-leg (ankle, tibia, fibula, and knee) to cause ACL rupture [5], visualized in Fig. 4(a). The current injury method emulated this model by compressing the lower-leg between the polystyrene platform and the device, visualized in Fig. 4(b).

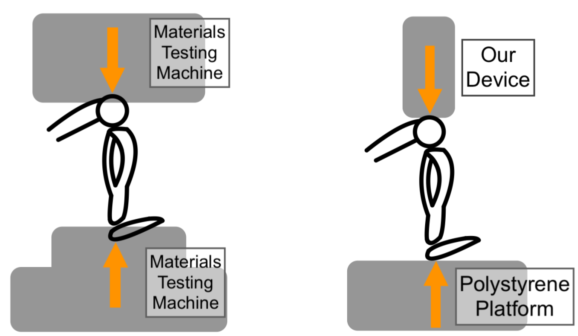


(a) Christiansen, et al.  (b) The current study

Fig. 4: Force delivery setup comparison

As a preliminary study, euthanized mouse specimens (*n=4*) were secured on a polystyrene platform with electric tape. In order to observe the integrity of the skin, the leg was rid of hair via a human-grade hair removal product. The device was aligned axially with the lower leg. Force was applied gradually at the knee axially until a ”pop” was heard or felt by the user, indicating ACL rupture. The ”pop” was heard consistently in each injury. After the injury was complete, each knee was dissected and inspected for ACL integrity and surrounding tissue damage. Table II shows that out of the 8 legs, 5 legs were injury samples and 3 legs were sham injury samples. 4 out of 5 injury samples were identified as ACL ruptured, and 1 out of 5 was inconclusive. 3 out of 5 injury samples showed no identifiable surrounding macroscopic tissue damage, and 2 out of 5 was inconclusive. The preliminary study indicated no signs for failure of effective emulation.

TABLE II: PRELIMINARY INJURY STUDY

| Mouse | Leg | Injury/Sham | ACL Integrity | Surr. Damage |
|---|---|---|---|---|
| 1 | Left | Injury | Ruptured | Absent |
| | Right | Sham | Intact | Absent |
| 2 | Left | Sham | Intact | Absent |
| | Right | Injury | Ruptured | Absent |
| 3 | Left | Injury | Inconclusive | Inconclusive |
| | Right | Sham | Intact | Inconclusive |
| 4 | Left | Injury | Ruptured | Absent |
| | Right | Injury | Inconclusive | Inconclusive |

Anesthetized mice (*n=209*) were subject to the same injury method as the euthanized mouse specimens in the preliminary study. After the injury was complete, instead of dissecting the knee, Lachman test was performed on the specimens. A positive Lachman test is evidence of ACL tear. If the Lachman test was negative, the injury attempt was repeated until the test was positive.

The Lachman test is carried out with the mouse knee bent to about 15°. The femur is stabilized, and the tibia is pulled forward. A steady restraint to anterior movement is considered as a normal response. Anterior displacement of proximal tibia is felt by the examiner's thumb to determine the result of the Lachman test. Anesthesia has shown to increase the accuracy of the Lachman test [8].

## III. RESULTS

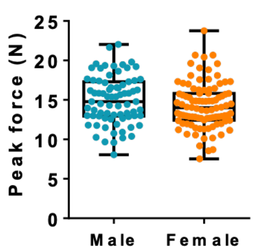


Fig. 5: Male vs. female load at ACL rupture

Of the 209 anesthetized specimens, 41 were excluded due to: (a) multiple attempts at ACL injury caused by negative Lachman tests, (b) unexpected behavior from the device which resulted in random graphs. The exclusion was done in order to achieve consistency. A total of 168 specimens were included. The loads at ACL rupture for specimens with multiple injury attempts had a mean within one standard deviation (SD) of the single injury attemps.

The mean load at ACL rupture was 14.62 N ($\sigma = 3.00N$) for all mice. For males and females, the mean load at ACL rupture was 14.98 N ($\sigma = 3.06N$) and 14.25 N ($\sigma = 2.92N$) respectively. Fig. 5 provides a visual contrast between males and females. Fig. 6 includes four representative graphs for the included samples. A gradual increase of force over time can be observed, which is ceased by ACL rupture at the maximum value of the curve. Table III shows the mean values of load at ACL rupture for left and right legs.

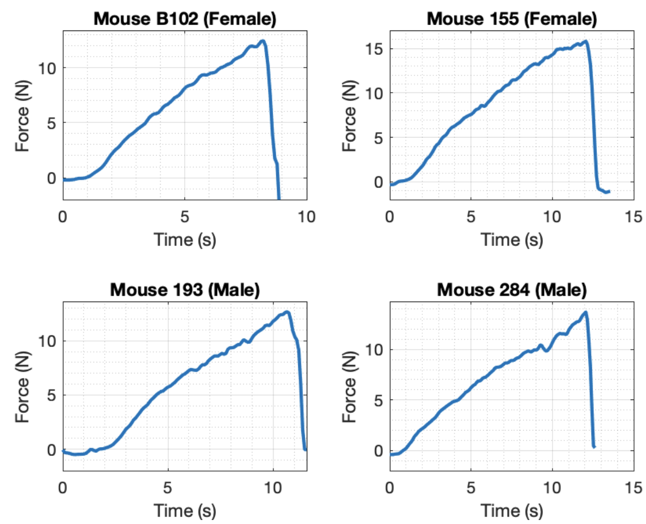


Fig. 6: Representative graphs for ACL injury

TABLE III: LOADS AT ACL RUPTURE

| Sex | Leg | Mean (N) | SD (±) |
|---|---|---|---|
| Male | Right | 13.88 | 2.68 |
| | Left | 15.69 | 3.29 |
| Female | Right | 13.88 | 2.81 |
| | Left | 14.56 | 3.01 |

## IV. DISCUSSION

### A. *In Vivo Mouse ACL Injury Study*

The calibration regression is decisively linear and the results of the *in vivo* injury test are highly similar to other ACL injury graphs in the literature [4]. This indicates successful emulation of the injury model developed by Christiansen et al. The mean force at ACL rupture is comparable to that of previously published results. Furthermore, previous studies have indicated no differences between male and female specimens in load at ACL rupture [4]. Similarly, in the current study, no difference between males and females was found.

## B. Theory

The aluminum beam (see Materials and Methods) experiences strain when it experiences a couple loading. This results in a moment ($M$), which causes bending stress ($\sigma$):

$$\sigma = -\frac{My}{I} \tag{2}$$

where $I$ is the area moment of inertia and $y$ is the distance from the neutral axis to the location of interest, which is the outer surface of the beam where two strain gauges are located. The bending stress can be converted to strain ($\epsilon$):

$$\epsilon = -\frac{\sigma}{E} \tag{3}$$

for a material with modulus of elasticity $E$.

## C. Design Parameters

*1) Circuit:* A Wheatstone bridge was used to quantify strain (Fig. 2). The resistance of a strain gauge is affected by ambient temperature. However, a circuit that uses a half-bridge design is not affected by variation in temperature because both resistors have equal changes in resistance, resulting in no net change in voltage.

Strain results in a small ($\leq 1\Omega$) resistance change in the circuit with high noise and low resolution. The HX711 load cell amplifier was integrated into the circuit in order to overcome this problem, resulting in a high resolution signal with low noise.

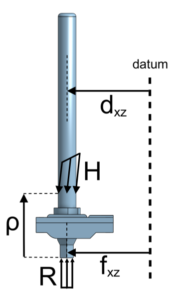


(a) Forces on device.

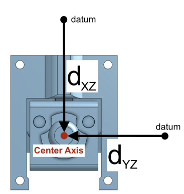


(b) Displacement between central axis and datums

Fig. 7: Force diagrams

*2) Mechanical Parts:* 3D printed mechanical parts were designed to provide maximum stability during load delivery. Stability is determined by two moments. In Fig. 7(a), force $H$ is the force applied by the hand and $R$ is the reaction force opposing the vertical component of $H$. $H_{xy}$ is the projection of $H$ onto the xy-plane. Displacements (a) $d_{xz}$ and (b) $f_{xz}$ are between the vertical datum and central axis of the (a) handle and (b) extruded tip respectively. Displacement $\rho$ originates from the reaction and terminates at the hand. Equation (4) shows that stability is maximized when $\rho$ is minimized.

$$\vec{M_1} = \vec{\rho} \times \vec{H_{xy}} \tag{4}$$

In Fig. 7(b), $d_{xz}$ (also shown in Fig. 7(a))and $d_{yz}$ are parallel to the xy-plane and they originate at datums and terminate at the central axis of the handle. Analogously, $f_{xz}$ (also shown in Fig. 7(a)) and $f_{yz}$ originate at the datums and terminate at the central axis of the extruded tip. Defining $\vec{d} = \vec{d_{xz}} + \vec{d_{yz}}$ and $\vec{f} = \vec{f_{xz}} + \vec{f_{yz}}$, the displacement between the central axes of the handle and extruded tip is quantified by $\vec{\Delta} = \vec{d} + \vec{f}$. The second moment can be minimized by designing coincident the central axes, resulting in maximum stability.

$$\vec{M_2} = \vec{\Delta} \times \vec{R} \tag{5}$$

## D. Clinical Relevance

The current study has implications for the future use of *in vivo* ACL injury models for osteoarthritis (OA). It incorporates traumatic loading as a more realistic mode contributing to the progression of OA compared to surgical models. The model of the current study, similar to other non-invasive models, initiates joint degeneration by inducing a localized osteoarthritic joint injury through mechanical impact [9]. This is not always achievable in the surgically induced injuries (invasive). Therefore, non-invasive models are more advantageous due to better replication of human acute processes initiated by ACL rupture caused by mechanical external injuries [5].

Our model may be used to study the effects of early treatments following injuries. Additionally, the portable aspect of our model opens doors to a high variety of *in situ* applications. The device in our model can be characterized as a low-cost DIY alternative to other models with well-written documentation, suggesting higher accessibility compared to other non-invasive models.

## E. Limitations

Although results indicated that the device is consistent and reliable, a commercial-grade materials testing machine is more reliable. Furthermore, the standard deviation for the mean ACL rupture load was higher than other studies. This may be due to imperfect emulation of other non-invasive injury models.

# V. Conclusion

Our model is a reliable and consistent alternative to other non-invasive ACL injury models which primarily use materials testing machines. *In vivo* ACL injury experiments have successfully reproduced the findings of other studies. Digital output of the device has shown a decisively linear relationship to the load applied.

# Acknowledgment

The authors would like to thank Ashley Proctor for performing the ACL injury with earlier prototypes of the device. The authors would like to thank Ahmet Selcuk Can for providing access to 3D printing equipment and ordering electronic parts. Funding sources had no involvement in study design, data acquisition, interpretation or manuscript preparation.

# REFERENCES


[1] S. M. Gianotti, S. W. Marshall, P. A. Hume, and L. Bunt, “Incidence of anterior cruciate ligament injury and other knee ligament injuries: A national population-based study,” Journal of Science and Medicine in Sport, vol. 12, no. 6, pp. 622–627, Nov. 2009.

[2] N. A. Friel and C. R. Chu, “The Role of ACL Injury in the Development of Posttraumatic Knee Osteoarthritis,” Clinics in Sports Medicine, vol. 32, no. 1, pp. 1–12, Jan. 2013.

[3] M. H. Gregory, N. Capito, K. Kuroki, A. M. Stoker, J. L. Cook, and S. L. Sherman, “A Review of Translational Animal Models for Knee Osteoarthritis,” Arthritis, vol. 2012, pp. 1–14, Dec. 2012.

[4] C. L. Blaker, C. B. Little, and E. C. Clarke, “Joint loads resulting in ACL rupture: Effects of age, sex, and body mass on injury load and mode of failure in a mouse model,” J. Orthop. Res., vol. 35, no. 8, pp. 1754–1763, Sep. 2016.

[5] B. A. Christiansen, M. J. Anderson, C. A. Lee, J. C. Williams, J. H. N. Yik, and D. R. Haudenschild, “Musculoskeletal changes following non-invasive knee injury using a novel mouse model of post-traumatic osteoarthritis,” Osteoarthritis and Cartilage, vol. 20, no. 7, pp. 773–782, Jul. 2012.

[6] T. Maerz, M. D. Kurdziel, A. A. Davidson, K. C. Baker, K. Anderson, and H. W. T. Matthew, “Biomechanical Characterization of a Model of Noninvasive, Traumatic Anterior Cruciate Ligament Injury in the Rat,” Ann Biomed Eng, vol. 43, no. 10, pp. 2467–2476, Mar. 2015.

[7] N. Y. Can, “STIF-2019,” https://github.com/ncan33/STIF-2019

[8] H. Makhmalbaf, A. Moradi, S. Ganji, F. Omidi-Kashani, “Accuracy of lachman and anterior drawer tests for anterior cruciate ligament injuries,” Arch Bone Jt Surg, vol. 1, no. 2, pp. 94–97, Dec. 2013.

[9] B. Poulet, R. W. Hamilton, S. Shefelbine, and A. A. Pitsillides, “Characterizing a novel and adjustable noninvasive murine joint loading model,” Arthritis and Rheumatism, vol. 63, no. 1, pp. 137–147, Dec. 2010.